




Practical empirical estimation of evaporation for mining and industrial water balances: application to a South African process dam

Marita Johanna Pretorius and Ione Loots   *

Department of Civil Engineering, University of Pretoria, Lynnwood Road, Hatfield, Pretoria, South Africa

*Corresponding author. E-mail: ione.loots@up.ac.za

 IL, 0000-0003-0715-6852

ABSTRACT

Direct measurement of evaporation at mining and industrial sites is highly accurate, but often prohibitively expensive, limiting its routine use in operational water balance modelling. This study evaluates a practical, cost-conscious approach for estimating daily evaporation using commonly applied empirical methods. Model performance was assessed by comparison with measured evaporation at both daily and aggregate scales. Among the methods tested, the Hargreaves equation provided a simpler yet sufficiently accurate alternative to the Penman–Monteith equation for operational applications. Sensitivity analysis showed that temperature is the dominant control on evaporation estimates for both methods, while solar radiation additionally influences Penman–Monteith estimates. Prioritising temperature and solar radiation measurements can substantially improve evaporation estimates where monitoring resources are limited. Local rainfall and wind measurements remain necessary to account for spatial variability and non-modelled losses. The results demonstrate that reliable evaporation estimates can be achieved using simplified empirical methods, supporting improved water balance assessments at mining and industrial sites where direct measurements are not feasible.

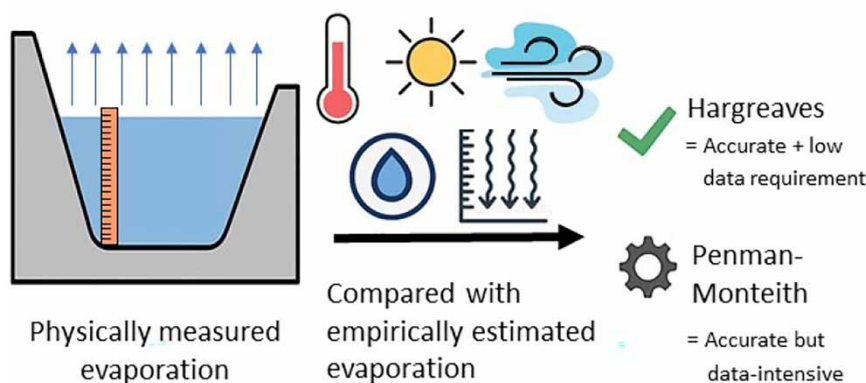
Key words: evaporation, Hargreaves, Penman–Monteith, Priestley–Taylor, solar radiation, water resource management

HIGHLIGHTS

- The Penman–Monteith and Hargreaves methods can accurately estimate evaporation in process dams.
- The Hargreaves method is a practical, low-cost alternative requiring fewer inputs and simpler computation.
- Accurate measurement of temperature and solar radiation is critical.
- Prioritising key parameters enables reliable estimates under budget constraints.

GRAPHICAL ABSTRACT

Practical Evaporation Estimation Using the Hargreaves Method



This is an Open Access article distributed under the terms of the Creative Commons Attribution Licence (CC BY 4.0), which permits copying, adaptation and redistribution, provided the original work is properly cited (<http://creativecommons.org/licenses/by/4.0/>).

1. INTRODUCTION

1.1. Background

Water security is a growing concern, especially in regions where water resources are limited and where the water demand may exceed the supply for certain periods (Arora & Mishra 2022; Leonard 2023). Mining and industrial operations rely on water for various processes, such as cooling, mineral processing, and dust suppression. Effective water management is required to sustain these operations, and knowledge of their water balance is required. Evaporation is one critical aspect that contributes to the loss of water and therefore influences the water availability from a process dam and other open water bodies (Van Dijk & Van Vuuren 2009; Pillco Zolá *et al.* 2019; Tian *et al.* 2021; Nevermann *et al.* 2024).

Evaporation is a complex phenomenon determined by several meteorological and surface variables (Shuttleworth 2007; Miralles *et al.* 2020). Many studies have investigated evaporation internationally, with some estimating evaporation at a global scale (e.g. Brutsaert *et al.* 2020; Tian *et al.* 2022). However, in South Africa, limited previous studies have been conducted to determine average evaporation (e.g. Schulze *et al.* 2008; Schulze 2011; Bailey & Pitman 2015). These studies determined evaporation at monthly or annual scales and provide evaporation maps for the entire country, often with large variations in the reported average evaporation.

1.2. Problem statement

Mining and industrial entities often calculate their water balance on a daily timestep and thus need daily evaporation rates. Evaporation estimation techniques can be broadly categorised into empirical and physical methods (Dubovský *et al.* 2021; Lindauer *et al.* 2023). Physical methods use water level readings from water bodies or eddy covariance techniques to determine observed evaporation (Lindauer *et al.* 2023). Physical evaporation measurements are conducted around South Africa with evaporation pans such as the A-pan or S-pan (Chapman *et al.* 2021). The S-pan is the standard used by the Department of Water and Sanitation in South Africa and is deployed at large dams (Braune 2020).

Empirical methods use meteorological parameters to estimate daily evaporation through mathematical equations. The parameters vary per method, but broadly include temperature, solar radiation, wind speed, relative humidity, and atmospheric pressure (Yaseen *et al.* 2020; Dubovský *et al.* 2021; Santos *et al.* 2022; Lindauer *et al.* 2023). Numerous mathematical methods have been developed since the 1800s (Dubovský *et al.* 2021), and previous studies have compared the accuracy of various empirical methods, with many focussing on land surface evaporation (e.g. Crago & Brutsaert 1992; Tabari *et al.* 2013; Han *et al.* 2024) and other studies comparing the methods in lake or reservoir evaporation studies (e.g. Majidi *et al.* 2015; Patel & Majmundar 2016; Pillco Zolá *et al.* 2019; Dubovský *et al.* 2021; Santos *et al.* 2022; Lindauer *et al.* 2023). However, to the authors' knowledge, no previous studies focussed specifically on the interior highveld of South Africa.

The Penman–Monteith (PM) method is considered the standard method for calculating land surface evaporation (Allen *et al.* 1998; Dubovský *et al.* 2021) and can be adapted to calculate open body evaporation using an albedo factor (also known as the reflection coefficient) representing open water surfaces rather than vegetation (Jensen *et al.* 2005). Due to the amount of data included in this method, it provides accurate results in various regions and climates (Dubovský *et al.* 2021). Other methods, such as the Hargreaves and Priestley–Taylor (PT) methods, are simpler to apply (Lindauer *et al.* 2023). If a simple method were to produce similar evaporation estimations for process dams in South Africa, then mining and industrial entities would require less input data for water balance calculations. This justifies the inclusion of simple methods in a study on applicable evaporation methods in the region.

As observed by Dlouhá *et al.* (2021a), in practical applications, it is not always possible to measure all of the meteorological input parameters. This is especially true in resource-constrained regions such as South Africa. Therefore, the sensitivity of different mathematical evaporation estimation methods to different meteorological parameters would need to be determined to guide mining and industrial entities on where to focus efforts for accurate data collection.

Furthermore, the reliability of empirical evaporation calculations is intrinsically linked to the accuracy and validity of the meteorological data sources. Meteorological data can be obtained from multiple sources, including on-site measurement locations and commercially available data. Climate conditions can vary per geographical location, leading to variations in the observed and measured parameters. In many cases, industrial entities would be able to save money and resources if they could purchase meteorological data from commercial sources.

However, no previous work has been done in the region to determine the required proximity of commercial weather stations to study sites, in order to justify their use for evaporation calculation at a daily timescale.

1.3. Aim and objectives

Therefore, this study aims to address this research gap by providing a practical approach to calculate sufficiently accurate daily evaporation for mining or industrial water balance determination with simple empirical methods. The first objective is to compare empirically calculated evaporation with physically measured evaporation in a long-term storage dam to determine the most applicable methods. The second objective is to determine the sensitivity of applicable empirical methods to different meteorological parameters. The final objective is to quantify the influence of instrumentation proximity to the study site on the meteorological parameters used for evaporation calculations.

2. METHODS

2.1. Study area

The study area is located in the interior highveld region of Mpumalanga, South Africa, at an altitude of approximately 1,600 m above mean sea level. It experiences long, hot summers and short, cool, winters. Precipitation occurs mainly between October and April as summer thunderstorms, with a mean annual precipitation of approximately 615 mm (Smithers & Schulze 2003). Table 1 shows the estimated annual evaporation rate for this study's area of interest, based on each of the previous South African studies. The range of mean annual evaporation reported in the study area is between 1,400 and 2,200 mm. This represents a significant discrepancy of over 50% between studies, and therefore further investigation into site-specific evaporation is warranted.

Table 1 | Mean annual evaporation for the study area, as reported in previous studies

Source	Evaporation determination	Mean annual evaporation (mm)
Schulze <i>et al.</i> (2008)	A-pan equivalent	2,000–2,200
Schulze (2011)	Penman–Monteith	1,400–1,600
Bailey & Pitman (2015)	A-pan at locations throughout the country, with results interpolated	2,000–2,200
Bailey & Pitman (2015)	S-pan at locations throughout the country, with results interpolated	1,500–1,600

The study site was selected for its fully lined earth dam that is used as a long-term storage dam. Due to the lining, the seepage from this dam can be taken as negligible (Finch & Hall 2001). The dam level is monitored daily, allowing verification of empirically calculated evaporation against a dam volume prediction method. Low and infrequent inflow and outflow volumes in this dam minimise uncertainty in the water balance method for determining evaporation. On-site and commercial meteorological data, collected within 6 km of the dam, support the empirical calculation of evaporation. The relative locations of the dam and weather stations are shown in Figure 1.

2.2. Water level measurement

The dam water levels are measured in two ways. The first level measurement method is done manually with surveying equipment at weekly intervals. A Trantech 4–20 mA pressure sensor is also installed in the dam, automatically measuring in 15-min intervals and to an accuracy of 1 mm. The pressure sensor cables are connected to the data loggers and are placed inside the dam at a depth of between 1.5 and 3 m.

2.3. Meteorological parameter acquisition

Evaporation is determined empirically using five parameters measured at meteorological stations: temperature, solar radiation, atmospheric pressure, wind speed, and relative humidity. An additional meteorological parameter, rainfall, was also evaluated, as it is used in physically based evaporation estimation and water balance calculation. As shown in Figure 1, several weather stations are located around the dam. The three manual (M) stations are only used to record rainfall data, but several other meteorological parameters are measured at the other 10 stations on the site (A1–4, C1–4, and P1–2). The commercial weather station is owned and operated

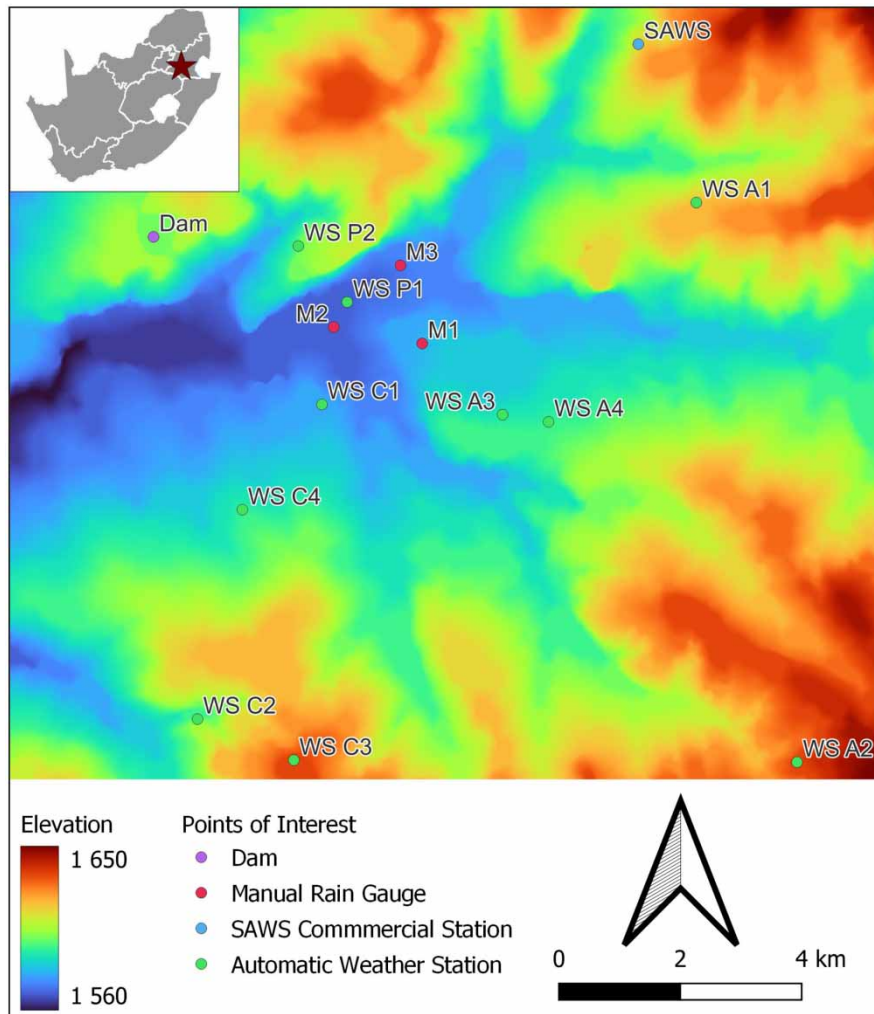


Figure 1 | Relative locations and elevation above mean sea level of the dam and weather stations used for this study, to show instrument proximity to the long-term storage dam used for water level measurement.

by the South African Weather Service (SAWS) within a 6 km radius of the site. The meteorological parameters measured at each station are listed in Table 2. The study period extends from June 2023 to September 2024. As some weather stations were not operational for the full period, relevant analyses were run for the longest possible periods with no data gaps. A dry period with no rainfall occurred from 18 April to 25 September 2024. This dry period was considered beneficial for the study and was used for the empirical method analysis, as the dam water level was not influenced by rainfall during this period.

The three manual stations measure rainfall depth with regular conical rain gauges. These were measured daily in the mornings at the same time each day, at 09:00 am. The automatic weather stations are fitted with the following instruments:

- A temperature (T) probe and a relative humidity (RH) probe are used to measure the named parameters. The relative humidity probe is a capacitance type, whilst the temperature probe is a resistance temperature detector type.
- A wind monitor is installed, consisting of a four-blade helicoid propeller to capture wind direction as well as wind speed.
- Solar radiation is measured by a pyranometer equipped with a silicon photovoltaic detector.
- An installed barometric pressure sensor is used, with a weatherproof enclosure for protection. This barometric pressure sensor measures atmospheric pressure. Its weatherproof enclosure protects it from dynamic pressure errors due to wind activity.

Table 2 | Meteorological parameters measured at each weather station

Station	Temperature	Solar radiation	Atmospheric pressure	Relative humidity	Wind speed & direction	Rainfall
WS A1	X		X		X	X
WS A2		X				
WS A3	X		X	X		
WS A4					X	
WS C1	X	X		X	X	
WS C2	X	X		X	X	X
WS C3	X	X		X	X	
WS C4	X	X		X	X	
WS P1		X			X	X
WS P2	X	X		X	X	X
M1						X
M2						X
M3						X
SAWS	X		X	X		X

- An automatic tipping bucket rain gauge is used. It is fitted with a bird wire assembly to discourage birds from sitting and nesting on the funnel rim.

2.4. Data cleaning and validation

Incorrect meteorological data can cause one to overestimate or underestimate empirically calculated evaporation, potentially leading to wrong decisions regarding managing the water body. Therefore, data validation was conducted on all measured meteorological parameters. The weather measurement devices in the study area are calibrated annually. Even when a device has been calibrated, a certain degree of data validation is still necessary, as errors that can impact the measured data may arise. Typical errors that can occur are sorted into three categories (Abtew & Melesse 2013), namely, systematic errors (caused by equipment manufacturing defects or calibration errors, which can cause a constant up or downwards drift); random errors (errors that occur randomly with the cause unknown, with no apparent pattern. It could be due to equipment defects, instrument limitations, instrument calibration and programming, data recording, transfer, processing, and storage methods); or Process errors (through data recording, transfer, processing, and storage methods). Data correction methods implemented in this study include the removal of incorrect data and replacing them, as applicable, with zero values (for example, rainfall measured during instrument calibration), or replacement with the last correct value (for example, atmospheric pressure or dam levels), or a comparable value (for example, long periods of missing data for solar radiation). Another check conducted was to ensure that the recorded meteorological parameter values fell within predefined bounds, such as solar radiation.

2.5. Evaporation calculation methods

2.5.1. Physical evaporation measurement

Physical evaporation was estimated using a simplified water balance approach based on the definition by Maidment (1993), who defines potential evaporation as ‘the quantity of water evaporated per unit area, per unit time from an idealised, extensive free water surface under existing atmospheric conditions.’ A similar approach was also adopted in Dlouhá *et al.* (2021b), where they took evaporation from a lake as being precipitation plus artificial inflow minus the water level change. In this study, the effect of rainfall was minimised by restricting the analysis to the dry period from 18 April to 25 September 2024. Due to the dam being lined, seepage did not need to be incorporated. No artificial inflows or outflows were recorded during this period. Where the water level increased due to minor precipitation events, the evaporation was assumed to be zero, consistent with the approach of Maidment (1993). Therefore, evaporation during the dry period (when negligible precipitation, no artificial inflow or outflow, and no seepage was recorded)

was calculated as the difference between the recorded water level on a given day and that of the preceding day, as presented in the following equation:

$$E = \max(\text{Water level}_{\text{preceding day}} - \text{Water level}_{\text{current day}}, 0) \quad (1)$$

where E is the evaporation rate (mm); $\text{Water level}_{\text{preceding day}}$ is the water level in the dam for the preceding day (mm); and $\text{Water level}_{\text{current day}}$ is the water level in the dam for the current day (mm).

2.5.2. Empirical evaporation methods

Various empirical equations have been developed since the 1940s, with Meyer (1944) developing one of the first methods to determine evaporation based on mass transfer. The method estimates evaporation (E) based on the difference between saturated vapour pressure at the water surface (e_s) with the vapour pressure at 2 m above the surface (e_a), along with wind speed at a reference height of 7.6 m ($u_{7.6}$) (Equation (2)):

$$E = C \left(1 + \frac{u_{7.6}}{16.09} \right) (e_s - e_a) \quad (2)$$

Another method used in South Africa and internationally, the Linacre method (Linacre 1977; Santos *et al.* 2022), estimates evaporation by calculating the sea-level equivalent temperature (T_m) of the measured mean temperature (T_{mean}) by utilising the dew point temperature (T_d). It considers the physical location of the site by considering the latitude (φ), shown in the following equation:

$$E = \frac{((700 T_m)/(100 - \varphi)) + 15(T_{\text{mean}} - T_d)}{80 - T_{\text{mean}}} \quad (3)$$

The widely used Hargreaves method, also known as the Hargreaves–Samani method (e.g. Dlouhá *et al.* 2021a; Santos *et al.* 2022; Lindauer *et al.* 2023), determines evaporation with temperature data (Allen *et al.* 1998). Hargreaves suggested that evaporation (E) estimates should be conducted on a monthly averaging period by taking the difference between the mean monthly maximum and minimum temperatures ($\bar{\delta}_T$). He further used the water equivalent of extraterrestrial radiation (S_o) as well as daily air temperature (T) to calculate evaporation (Maidment 1993), as per the following equation:

$$E = 0.0023 S_o \bar{\delta}_T (T + 17.8) \quad (4)$$

Celestin *et al.* (2020) presented the Hargreaves model calculated on a daily timestep by using the daily mean, maximum, and minimum temperatures (T_{mean} , T_{max} and T_{min}), as well as extraterrestrial radiation (R_a) and the latent heat of vaporisation (λ), as shown in the following equation:

$$E = 0.0023 (T_{\text{mean}} + 17.8)(T_{\text{max}} - T_{\text{min}})^{0.5} R_a/\lambda \quad (5)$$

The Penman–Monteith (PM) method combines temperature and radiation-based techniques to calculate evaporation (Allen *et al.* 1998; Dubovský *et al.* 2021). It uses meteorological data, such as air temperature, solar radiation, relative humidity, wind speed, and atmospheric pressure. Solar radiation is used to calculate the net radiation that reaches the Earth (R_n) and subtracts the soil heat flux density (G) from this radiation. The slope of the saturation vapour pressure curve is presented by Δ_e . It calculates the saturation vapour pressure deficit ($e_s - e_a$) from relative humidity and temperature measurements, utilises wind speed at a 2 m reference height (u_2). It takes the daily air temperature (T) into consideration, and multiplies it by the psychrometric constant (γ), which is calculated from atmospheric pressure, as shown in the following equation.

$$E = \frac{0.408\Delta_e(R_n - G) + \gamma(900/T + 273)u_2(e_s - e_a)}{\Delta_e + \gamma(1 + 0.34 u_2)} \quad (6)$$

The PT method is a simplified version of the Penman–Monteith method (Shuttleworth 2007). The vapour deficit and convection terms are simplified to one empirical term, namely the PT constant, α (Mercer 2018). The PT method uses the net incoming solar radiation (R_n) and soil heat flux term (G), like the Penman–Monteith method

(Celestin *et al.* 2020). It further uses the slope of the saturation pressure curve (Δ_e), which is derived from temperature and relative humidity readings, the psychrometric constant (γ) derived from atmospheric pressure, as well as the latent heat of vaporisation (λ), which is a constant value, as included in the following equation:

$$E = \alpha (R_n - G) \left(\frac{\Delta_e}{\Delta_e + \gamma} \right) / \lambda \quad (7)$$

The Meyer and Linacre methods do not use solar radiation as an input, with the Meyer method based on mass transfer and the Linacre method being temperature-based. They were therefore included as simple methods to determine their applicability in the study area, since they have been used successfully in other studies in semi-arid (Patel & Majmundar 2016) and temperate (Santos *et al.* 2022) regions. The Hargreaves method was used in studies in other regions and found to give a good approximation of lake evaporation (Dlouhá *et al.* 2021a; Lindauer *et al.* 2023). For the Hargreaves method, solar radiation was estimated from temperature data, at a daily timestep. The Penman–Monteith method is often considered to be a benchmark to which other methods are compared (Allen *et al.* 1998; Dlouhá *et al.* 2021a), and it was therefore included as the benchmark method in this study, despite its data requirements. The Penman–Monteith (PM) and PT methods can be seen as combination methods, with the PT method representing a simplified version of the PM method, justifying its inclusion in the study. For both these methods, the solar radiation was applied in three ways: from temperature data, at a daily timestep ($^{\circ}\text{C}$), from direct solar radiation readings, at daily timesteps (daily R_s), and at hourly time-steps (hourly R_s). This selection of methods includes simple methods in line with the study aim to calculate sufficiently accurate daily evaporation for mining or industrial water balance determination with simple empirical methods.

2.5.3. Evaporation method evaluation

To evaluate the relevance of the empirical evaporation calculation methods and the physically based water balance method, the cumulative predicted volume for each method was compared to an actual observed volume of water in the dam, inferred from a water level reading, via a stage-volume graph. In turn, the stage-volume graph was generated by combining a bathymetric survey with an aerial survey of the dry section of the dam basin. The aerial survey supplemented the information not captured during the bathymetric survey.

The difference between the two methods was determined:

$$nS = S_{pr} - S_{act} \quad (8)$$

where nS is the difference between the actual and predicted dam volumes (ML); S_{pr} is the predicted dam volume (ML); and S_{act} is the actual dam volume (ML).

After confirming that the water balance method accurately captured evaporation during the dry period from April to September 2024, the root mean square error (RMSE), mean absolute error (MAE), and the mean bias error (MBE) statistical measures were used to evaluate the performance of the empirical evaporation methods in this study at a daily timescale. The equations are shown in Equations (9) to (11), with P_i denoting the predicted daily evaporation as calculated by each empirical method, O_i denoting the evaporation calculated using the simplified water balance method as a benchmark, and n being the number of data points.

$$\text{RMSE} = \sqrt{\frac{\sum_{i=1}^n (P_i - O_i)^2}{n}} \quad (9)$$

$$\text{MAE} = \frac{\sum_{i=1}^n |P_i - O_i|}{n} \quad (10)$$

$$\text{MBE} = \frac{\sum_{i=1}^n (P_i - O_i)}{n} \quad (11)$$

2.6. Isolating important parameter sets

Three approaches were used to isolate the most important meteorological parameter sets for empirical evaporation calculation in process dams: Pearson correlation analysis, main effects plots, and interaction plots. All three approaches were applied to the empirical evaporation methods that performed the best for the study area.

The widely used Pearson correlation coefficient (e.g. [Jana et al. 2016](#); [Zhang et al. 2017](#); [Al-Mukhtar 2021](#); [Abed et al. 2024](#)) was used at a significance level of 0.05 to determine the correlation between measured meteorological parameters and the empirically calculated evaporation. The strength of correlation was determined on a scale of -1 to $+1$ ([Montgomery & Runger 2010](#)), with labels as in [Table 3](#) (from [Schober et al. 2018](#)).

Table 3 | Pearson correlation coefficient interpretation ([Schober et al. 2018](#))

Pearson correlation coefficient (r)	Interpretation
0.00–0.10	Negligible correlation
0.10–0.39	Weak correlation
0.40–0.69	Moderate correlation
0.70–0.89	Strong correlation
0.90–1.00	Very strong correlation
1.00	Perfect correlation

The main effects plot is a graphical tool to visualise the impact of a single factor on the response variable in a factorial experiment ([Montgomery & Runger 2010](#)). The main effect is the average change in the response variable by changing the level of the single factor, whilst averaging over the levels of all other factors. For this study, the factors investigated were meteorological parameters (such as temperature, wind speed, etc.), with the response variable being the empirically calculated evaporation. The results were plotted and connected with a line. When the connected line is horizontal, the factor has no main effect on the response variable. When the line increases or decreases, there is a main effect. The steepness of the line slope indicates the magnitude of the impact ([Montgomery & Runger 2010](#)).

The main effects plots show how much a specific parameter affects the calculated evaporation. However, in some cases, the effect on evaporation is not solely due to the parameter investigated, but could be driven by a different parameter. The presence of these types of interactions is investigated with interaction plots. An interaction occurs when the effect of one factor on the response variable depends on the level of another factor ([Montgomery & Runger 2010](#)). Interaction plots visualise these relationships, helping one to determine whether the factors influence the response variable independently or jointly. With an interaction plot, one factor (A) is plotted on the horizontal axis versus the response variable on the vertical axis. Separate lines are drawn for each second factor (B) level, with level details in a legend. If the lines are parallel, there is no interaction, meaning the effect of A on the response is the same regardless of B's level. Non-parallel lines indicate interaction, as the effect of factor A depends on B.

2.7. Impact of instrument proximity on meteorological data

When meteorological data are obtained from commercial sources some distance away from the location of interest, the measurements will likely differ from those at the site. This study compared data from a commercial source with measurements taken at a specific site to assess the data's suitability for evaporation estimations compared to local data. Correlation analysis was conducted to describe these comparisons. The statistical analyses were conducted using a statistical software package called Minitab ([Barsalou 2015](#); [Minitab Statistical Software 2024](#)). The statistical formulas employed by Minitab have been cross-checked for validity by consulting statistical literature ([Montgomery & Runger 2010](#)).

Correlation analysis was used to quantify the differences between two or more stations that measure the same parameter. Covariance was used to measure the linear relationship between two variables ([Montgomery & Runger 2010](#)). It was used to indicate whether two variables simultaneously increase (positive covariance) or decrease (negative covariance). If no relationship exists, it will provide zero covariance. If the relationship between the two variables is non-linear, the covariance might not be able to detect the relationship. Covariance

can indicate whether the relationship is positive or negative, but it cannot demonstrate the strength of the relationship because the data is not standardised. To indicate the strength of a relationship, the Pearson correlation coefficient was used at a significance level of 0.05, with the strength of correlation coefficients as shown in Table 3.

3. RESULTS AND DISCUSSION

3.1. Finding applicable empirical evaporation calculation methods

The first objective is to compare empirically calculated evaporation with physically measured evaporation in a long-term storage dam to determine the most applicable methods. The aggregate performance of each evaporation method for the dry period is shown in Figure 2. The total evaporation calculated with each empirical method for the dry period from April to September 2024 is shown with the yellow bars, while the differences in calculated volume are shown in red for underestimation and blue for overestimation. From Figure 2, it is clear that the Meyer and Linacre methods performed significantly worse than other methods, with the Meyer method underestimating evaporation by approximately 300% and Linacre overestimating by almost 200%. The PT methods all underestimated the total evaporation by approximately 40%. The PM method, calculated at hourly timesteps and using measured solar radiation data, performed the best of the empirical methods. It was closely followed by the other two applications of the PM method and the Hargreaves method. The Water Balance Method predicts the evaporation almost perfectly. This was expected, as the Water Balance calculation uses the measured water level as an input. The slight discrepancy is attributed to cumulative calculation inaccuracy.

Method	Cumulative E error (nS)	Total E (mm for the dry period Apr – Sep 2024)
Meyer	107	182
PT (daily R_s)	58	343
PT ($^{\circ}\text{C}$)	56	349
PT (hourly R_s)	51	368
Hargreaves	20	466
PM (hourly R_s)	11	497
WBM (Dam)	4	542
PM (daily R_s)	19	592
PM ($^{\circ}\text{C}$)	20	595
Linacre	136	970

Figure 2 | Evaporation method performance for the dry period from Apr to Sep 2024, showing the overestimation of evaporation in blue, the underestimation of evaporation in red and total evaporation in yellow.

The statistical analysis of daily evaporation largely aligns with the results from the aggregate data, with the Hargreaves and PM methods performing the best across all three applied statistical measures (Table 4). Interestingly, the Hargreaves method has the lowest RMSE and MAE, followed by the PM method, calculated at hourly timesteps and using measured solar radiation data. The three PM methods have the lowest MBE, followed by the Hargreaves method. The Meyer and Linacre methods perform the worst when considering the daily data, with Meyer underestimating and Linacre overestimating daily evaporation, similar to the performance for aggregate data.

The good performance by the PM methods was expected, given that it is used as a benchmark method in various studies (e.g. Jensen *et al.* 2005; Dlouhá *et al.* 2021a). The performance of the Hargreaves method as a simple, yet sufficiently accurate alternative to the PM method also aligns with previous studies (Dubovský *et al.* 2021; Lindauer *et al.* 2023). In contrast to the results from previous studies (Patel & Majmundar 2016; Santos *et al.* 2022), the Meyer and Linacre methods perform poorly in this region, with Meyer severely underestimating

Table 4 | Statistical performance of the empirical versus the water balance method for daily evaporation during the study period from Apr to Sep 2024

Method	RMSE (mm/day)	MAE (mm/day)	MBE (mm/day)
Meyer	3.20	2.47	-2.24
PT (daily R_s)	2.66	2.00	-1.24
PT ($^{\circ}\text{C}$)	2.63	1.99	-1.20
PT (hourly R_s)	2.66	1.98	-1.09
Hargreaves	2.44	1.85	-0.48
PM (hourly R_s)	2.50	1.87	-0.28
PM (daily R_s)	2.53	1.94	0.31
PM ($^{\circ}\text{C}$)	2.52	1.94	0.32
Linacre	3.60	3.10	2.65

and Linacre severely overestimating evaporation. The underestimation of evaporation by the PT method is in line with expectation (Jensen *et al.* 2005).

Considering the data requirements and complex calculations for the PM and Water Balance methods, the Hargreaves method provides a practical, yet sufficiently accurate alternative for evaporation calculation and is recommended for use in the interior Highveld region of South Africa, in line with recommendations from other studies in temperate (Dubovský *et al.* 2021) and arid (Lindauer *et al.* 2023) regions. As calibration coefficients are not currently available for the region, it is recommended that future studies develop calibration coefficients for the Hargreaves method, as it represents a simple method that already works well in the region.

3.2. Isolating important parameter sets

The second objective is to determine the sensitivity of applicable empirical methods to different meteorological parameters, in order to guide mining and industrial entities on where to focus efforts for accurate data collection. The three analyses conducted in order to achieve this objective are described in this section.

3.2.1. Correlation analysis

The correlation between the measured parameters and empirically calculated evaporation was determined. Since the Hargreaves and PM methods performed best at calculating evaporation, the correlation coefficients were calculated for these two methods. The Pearson correlation coefficients between the measured meteorological parameters and the calculated evaporation are displayed in Table 5.

Table 5 | Pearson correlation coefficients for meteorological parameters vs evaporation

Calculation method	Relative humidity	Atmospheric pressure	Solar Radiation	Temperature (max)	Wind
Hargreaves	-0.325	-0.192		0.878	-0.008
PM (hourly R_s)	-0.728	-0.480	0.712	0.727	0.214

Temperature strongly correlates with evaporation for both methods, followed by solar radiation (although the Hargreaves method does not directly use this). The Pearson correlation coefficients suggest that the other measured parameters (relative humidity, atmospheric pressure, and wind speed) have a weak to negligible correlation with the Hargreaves evaporation (zero means no correlation). With the exception of the relative humidity, the PM method shows similar results.

3.2.2. Main effects analysis

'Main Effects' plots evaluate how the independently measured variables (temperature, solar radiation, relative humidity, atmospheric pressure, and wind speed) affect the dependent variable, evaporation. The main effects plot is shown for the Hargreaves method in Figure 3 and for the PM method (with hourly measured solar radiation) in Figure 4. The mean evaporation is plotted for each meteorological bin. The

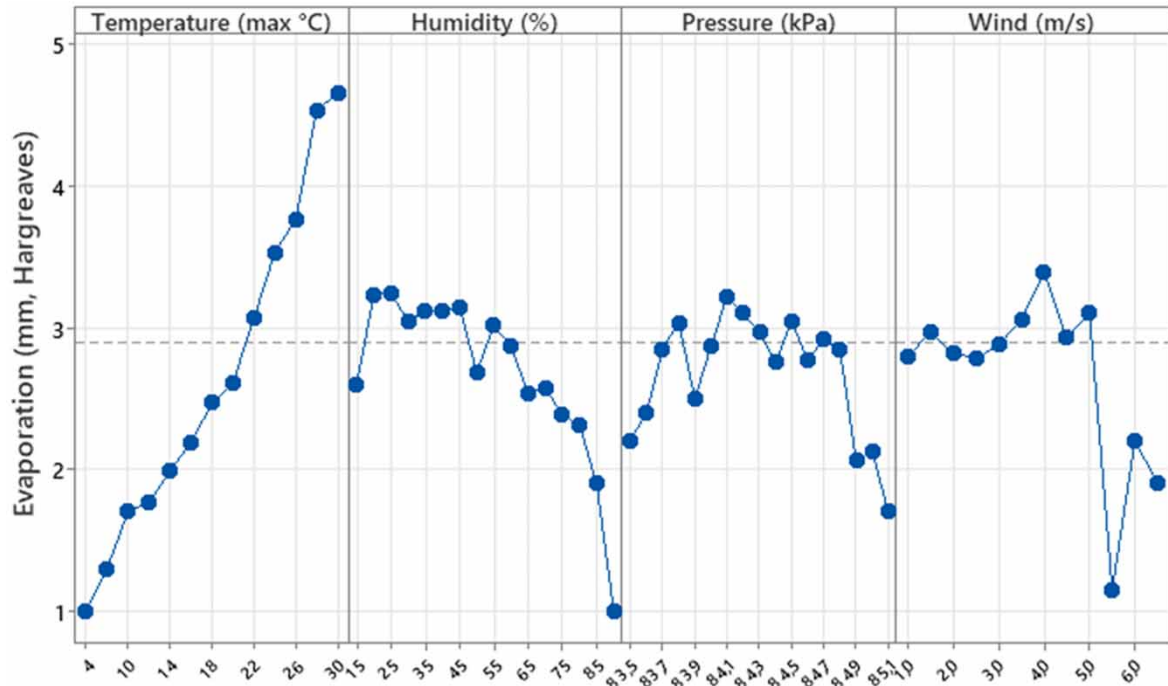


Figure 3 | Main effects plot for evaporation, Hargreaves method.

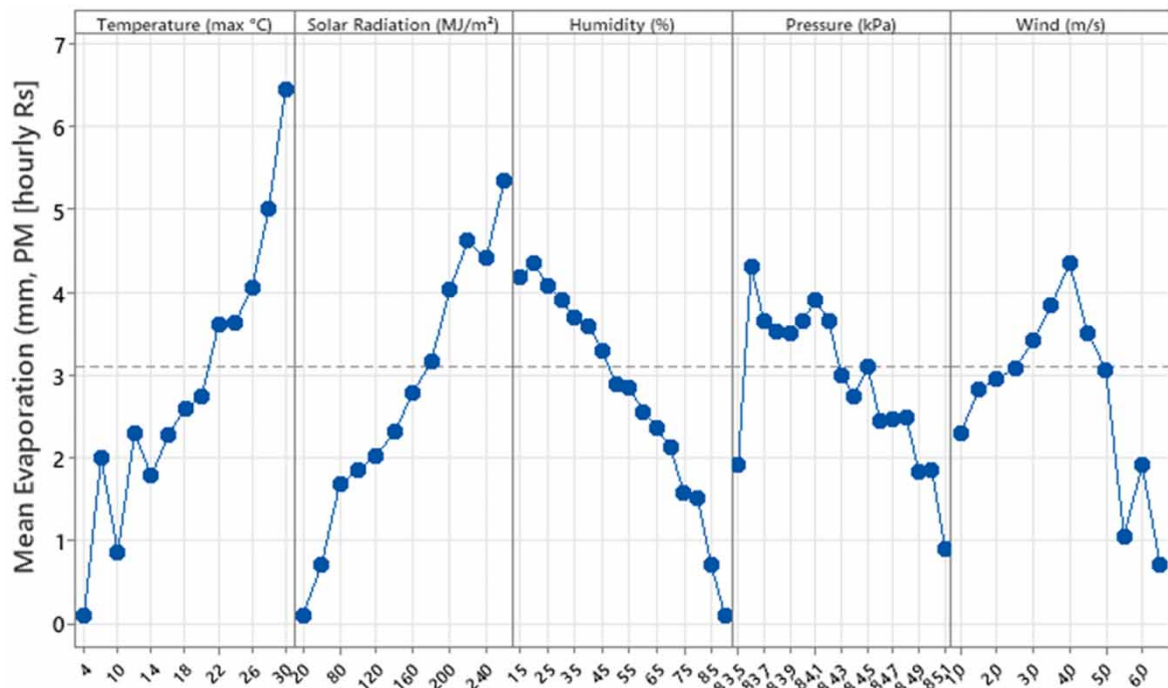


Figure 4 | Main effects plot for evaporation, PM (hourly R_s) method.

interactions between the measured variables and the calculated evaporation are visually illustrated. From these figures, it is clear that temperature and (for the PM method) solar radiation have the largest effect on calculated evaporation. Atmospheric pressure and wind speed have almost no effect on the outcome in either method.

3.2.3. Interaction plots

The main effect plots show how much a specific parameter affects the calculated evaporation. However, in some cases, the effect on evaporation is not solely due to the parameter investigated, but could be driven by a different parameter. Interaction plots were used to examine evaporation and maximum temperature at different levels of each of the other measured parameters. The results for the Hargreaves and PM methods were similar. As the Penman–Monteith method also uses solar radiation, the results for this method are shown in Figure 5. This figure shows a positive relationship between temperature and evaporation, for all of the corresponding wind [Figure 5(a)], atmospheric pressure (Figure 5(c)), relative humidity (Figure 5(e)), and solar radiation values (Figure 5(g)). Solar radiation also shows a positive relationship with evaporation at different temperatures (Figure 5(h)). But wind (Figure 5(b)), atmospheric pressure (Figure 5(d)), and relative humidity (Figure 5(f)) show relatively flat curves, indicating insignificant effects.

3.2.4. Insights on the isolation of important parameter sets

The correlation analysis results, main effects plots, and interaction plots all show that temperature has a significant influence on calculated evaporation when using the Hargreaves or PM methods. The temperature main effects and interaction plots show clear upward trends for both evaporation methods. This indicates that, as temperature increases, so does evaporation. A 2 °C increase in temperature means an increase of 0.5 mm evaporation at lower temperatures, and as the temperature increases, the corresponding evaporation can increase up to 1 mm per day. Figure 4 shows some noise at lower temperature readings. This sample size only spans the dry period from April to September 2024. During this period, there was only one reading for both 4 °C and 6 °C, and only two for 10 °C. With a larger sample size, these irregularities will likely smooth out.

Solar radiation is likewise shown to have a significant influence on calculated evaporation in the PM method. The Hargreaves method does not use the solar radiation parameter. The effect of solar radiation on the PM method is shown as having an upward trend in Figures 4 and 5. As solar radiation increases, so does evaporation.

Relative humidity shows a weak inverse relationship with evaporation for the Hargreaves method and a strong inverse correlation with the PM (hourly R_s) method. This means that as relative humidity increases, the calculated evaporation decreases, and vice versa. This is expected behaviour, as the relative humidity increases when the temperature decreases with a constant vapour pressure. With the Hargreaves method in Figure 3, the evaporation range only spans from 1 to 3.2 mm, a smaller range when compared to the PM method in Figure 4, with a range of 0–4.5 mm. This indicates that with the Hargreaves method, relative humidity has less influence on the calculated evaporation when compared to the PM method.

Both the correlation analysis results and the main effects plots indicate that wind speed and atmospheric pressure do not have a significant effect on calculated evaporation. Figures 3 and 4 show that the effect of wind speed is not linear. The evaporation is the highest when the measured wind speed is 4 m/s. The calculated evaporation sharply decreases with wind speeds higher than this, especially from 5.5 m/s upwards. This was attributed to colder temperatures associated with higher wind speeds. Further insight emerges when observing the interaction between temperature and wind speed (Figure 5(a) and 5(b)). The interaction is mainly driven by temperature, seen by the steep upward lines corresponding to rising temperatures in Figure 5(a). Wind speed also contributes to upward slopes until 4 m/s, though evaporation decreases at wind speeds higher than 4 m/s (Figure 5(b)). Wind has the added complexity that, with high wind speeds (>5 m/s), wave action can induce water loss, which is not accounted for mathematically. Therefore, local measurements are advised due to the variability of wind.

These results differ in some ways from findings in previous studies that focussed on evaporation from vegetated land surfaces. For example, Koudahe *et al.* (2018) found the PM method to be most sensitive to wind speed, maximum temperature, and solar radiation in humid and semi-arid areas. Jerszurki *et al.* (2019) concluded that vapour pressure deficit, calculated from relative humidity and temperature data, is the most sensitive parameter, followed by wind speed and solar radiation in tropical, subtropical, and semi-arid regions. Sabino & de Souza (2023) found the PM method to be most sensitive to solar radiation, followed by relative humidity and wind speed in grassland biomes. It is postulated that wind speed would have a more pronounced effect on vegetation than on open water surfaces, leading to the somewhat contradictory results in this study.

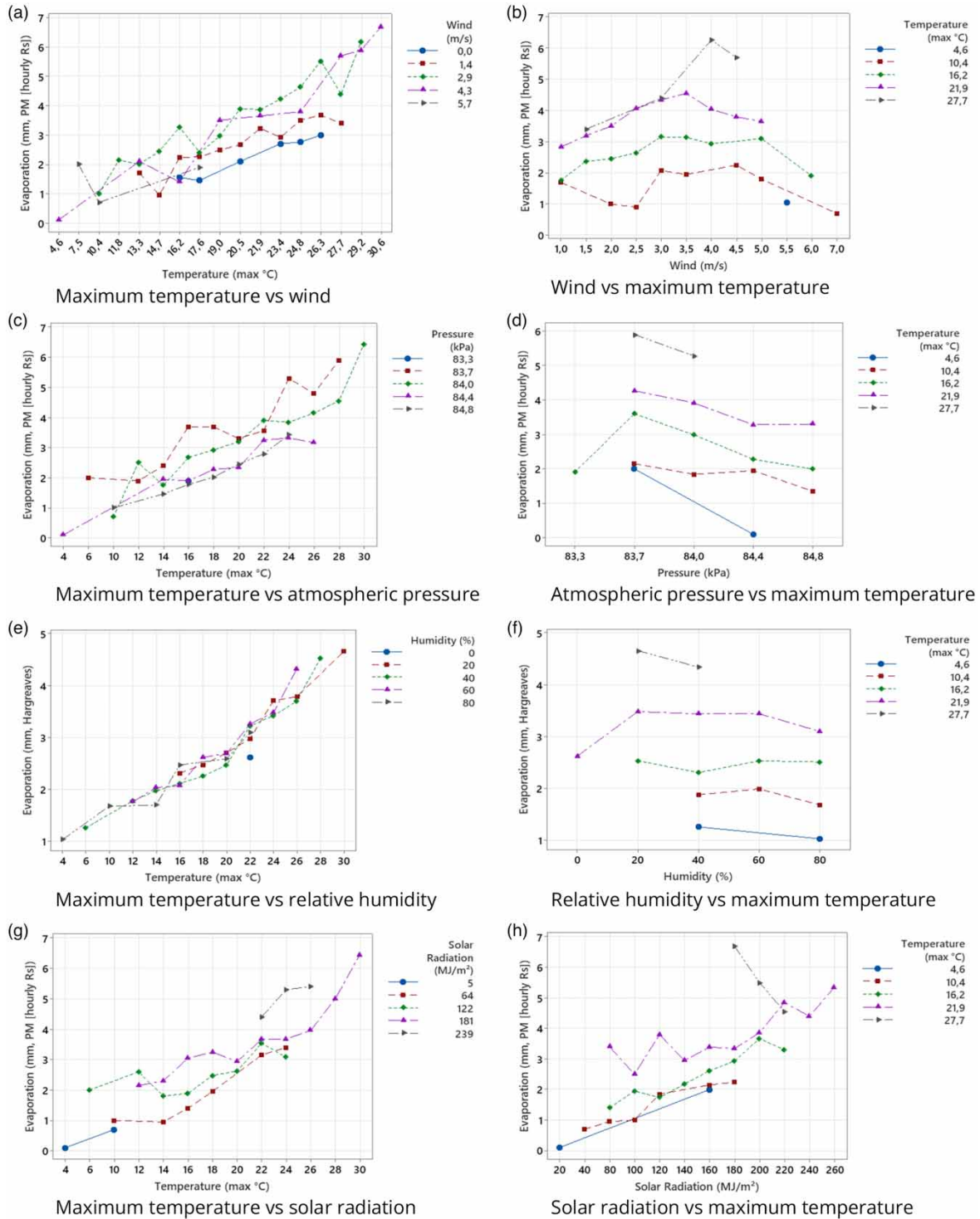


Figure 5 | Evaporation interaction plots for the Penman–Monteith method with hourly timesteps, using solar radiation, with the tested interactions shown underneath each plot (a)–(h). (a) Maximum temperature vs wind, (b) wind vs maximum temperature, (c) maximum temperature vs atmospheric pressure, (d) atmospheric pressure vs maximum temperature, (e) maximum temperature vs relative humidity, (f) relative humidity vs maximum temperature, (g) maximum temperature vs solar radiation, and (h) solar radiation vs maximum temperature.

3.3. Impact of instrument proximity on meteorological data

In order to achieve the final objective, the influence of instrumentation proximity on meteorological parameters had to be quantified. The Pearson correlation analysis results showed high degrees of correlation for most of the parameter sets. The 95% confidence interval (CI) of the Pearson correlation between the temperature datasets is

visually displayed in Figure 6 as an example of the results. In this example, all the datasets have a strong to very strong correlation (Schober *et al.* 2018). Similar results were found for solar radiation, relative humidity, and wind. These results are provided in the supplementary material.

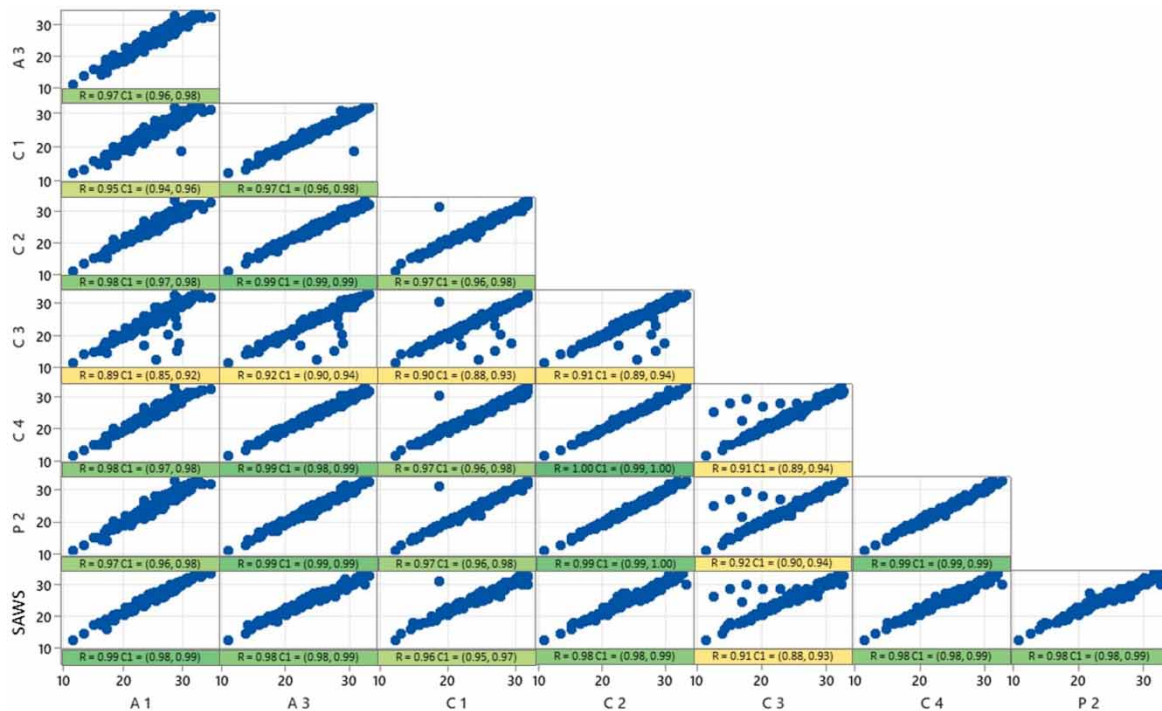


Figure 6 | Matrix of temperature scatter plots for 95% CI for Pearson correlation (January to June 2024), with colour-coded bars indicating the significance of correlation.

As deduced from the upward curve in the main effect plots for both the Hargreaves and PM methods, temperature impacts empirically calculated evaporation in this study area. Therefore, it is an important parameter to get as accurate as possible. Temperature data can be sourced commercially or measured locally with measurement devices. For the study area, the commercial SAWS temperature datasets have a very strong correlation with temperature readings from the site, although some periods with significant data gaps were found in the older data not included in the specific analysis. A service level agreement (SLA) is therefore recommended to ensure that the commercial entity (SAWS) reads the required stations consistently and maintains their instruments. Measuring temperature at multiple locations, provided there is no significant elevation difference or special topographical features in the vicinity, is not worth the financial investment.

Solar radiation readings significantly affect calculated evaporation in the PM method in this study area, as well as others (e.g. Koudahe *et al.* 2018; Jerszurki *et al.* 2019; Sabino & de Souza 2023). Local solar radiation measurements are recommended, as solar radiation readings are not always commercially available. Due to the measurement devices' inherent unreliability, a secondary station as a backup, with regular maintenance and calibration, is recommended when the PM method is used.

For the purposes of empirical evaporation calculation from storage dams, relative humidity, atmospheric pressure, and wind speed do not significantly influence the results in this study area, as shown through the correlation analysis, interaction plots, and main effects plots. However, local wind data is needed to account for non-mathematically modelled losses, such as those induced by wave action at high speeds, as experienced in the study area.

In contrast to the strong correlation for other meteorological parameter sets, the rainfall results showed a much wider range of correlation between datasets, as shown in Figure 7. The significant variation between gauges within a 6 km radius is consistent with the spatial distribution of convective rainfall in the region (e.g. Loots *et al.* 2023; Mouton *et al.* 2025). Two measurement methods were utilised: manual readings using a conical rain gauge and automatic readings from electronic tipping bucket gauges. SAWS correlates well (>0.8) with

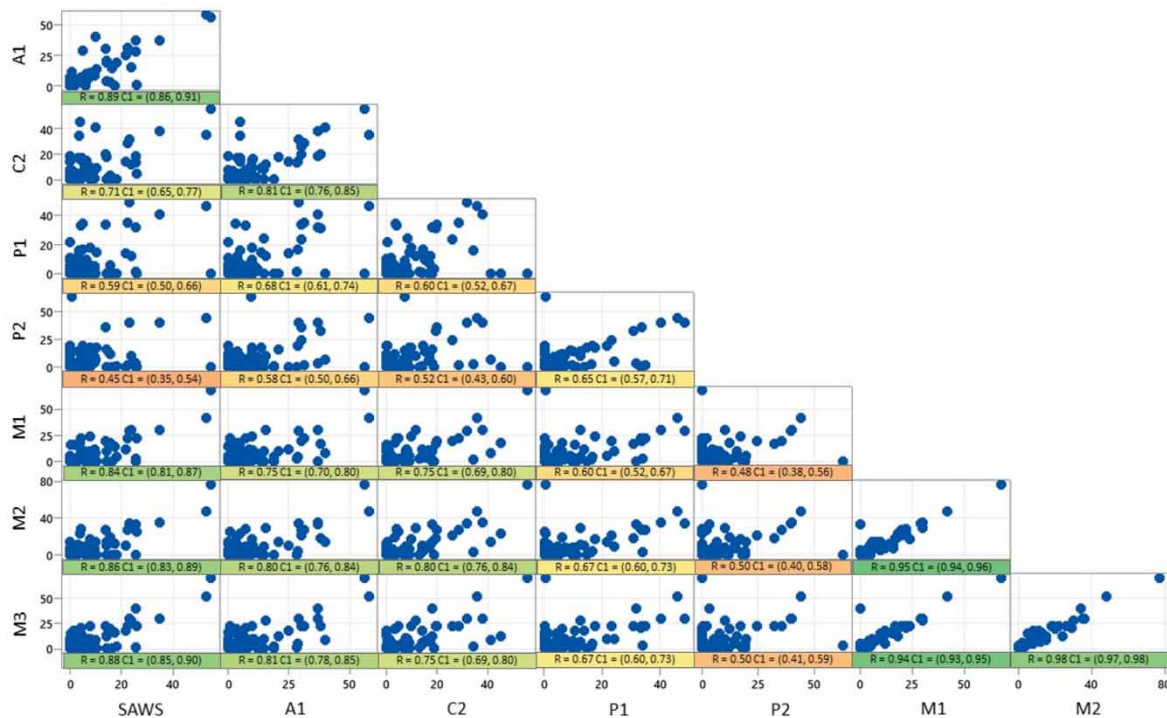


Figure 7 | Matrix of daily rainfall depth scatter plots for 95% CI for Pearson correlation (July 2023 to June 2024), with colour-coded bars indicating the significance of correlation.

the manual readings in the plant (M1 – M3). The manual readings (M1, M2, and M3) correlate very strongly (higher than 0.94).

Interestingly, the automatic rain measurements (A1, C2, P1, P2), taken at an 8.5 km distance from one another, only correlate moderately with one another (0.52–0.81). The automatic rain devices suffered from numerous data inaccuracies. Upon closer inspection of the data, it became evident that these devices sometimes measure rain after the rain event had stopped. In other cases, it stopped reading the rain altogether, probably caused by blockages. The manual readings gave more consistent measurements. In order to eliminate any possible errors in evaporation calculation due to erroneous rainfall data, the subsequent evaporation analyses were done for the dry period between April and September 2024.

Although empirical evaporation calculation methods do not directly incorporate rainfall in the equations, accounting for rainfall is important when considering long-term water balance. Therefore, rainfall is best measured on site and with reliable equipment, due to its high spatial variability.

4. CONCLUSIONS

Effective water resource management is critical for mining and industrial operations, particularly in water-scarce regions such as South Africa. The main aim of the study was to provide a practical approach to calculate sufficiently accurate daily evaporation for mining or industrial water balance determination with empirical methods. The Hargreaves method is recommended as a simple and practical method for calculating evaporation in the South African highveld region when solar radiation data is unavailable. When hourly solar radiation measurements are available, the PM method provides high-confidence evaporation estimations. Further studies would be required to confirm universal applicability.

Temperature was shown to have a significant effect on empirically calculated evaporation. Therefore, reliable temperature measurements are imperative for accurate evaporation calculation. Similarly, solar radiation significantly influences calculated evaporation for the PM method. Empirical evaporation calculation methods are less sensitive to relative humidity and atmospheric pressure changes than temperature when considering evaporation from dams.

Despite the sensitivity of the empirical methods to temperature data, within this study area, the measurements need not be taken at the site itself if a commercial station with reliable data is situated close to the site. Wind

speed variably influences calculated evaporation, depending on the calculation method used. Wind does have the added complexity that, with high wind speeds, wave action can induce water loss, which is not accounted for mathematically. Point rainfall also varies significantly within a small area. Therefore, local measurements are advised for both these parameters.

ACKNOWLEDGEMENTS

The South African Weather Service is gratefully acknowledged for providing meteorological data.

AUTHOR CONTRIBUTIONS

M.P. conceptualised the study, analysed the data, reviewed, and edited the article. I.L. wrote, reviewed, and edited the article.

DATA AVAILABILITY STATEMENT

Data cannot be made publicly available; readers should contact the corresponding author for details.

CONFLICT OF INTEREST

The authors declare there is no conflict.

REFERENCES

- Abed, M., Imteaz, M. A., Huang, Y. F. & Ahmed, A. N. (2024) Self-attention transformer model for pan evaporation prediction: a case study in Australia, *Journal of Hydroinformatics*, **26** (10), 2538–2255. <https://doi.org/10.2166/hydro.2024.104>.
- Abtew, W. & Melesse, A. (2013) *Evaporation and Evapotranspiration: Measurements and Estimations*. Dordrecht: Springer. <https://link.springer.com/book/10.1007/978-94-007-4737-1>.
- Allen, R., Pereira, L., Smith, M. & Raes, D. (1998) Crop evapotranspiration-guidelines for computing crop water requirements-FAO irrigation and drainage paper 56, *FAO, Rome*, **300** (9), D05109.
- Al-Mukhtar, M. (2021) Modeling of pan evaporation based on the development of machine learning methods, *Theoretical and Applied Climatology*, **146** (3), 961–979. <https://doi.org/10.1007/s00704-021-03760-4>.
- Arora, N. K. & Mishra, I. (2022) Sustainable development goal 6: global water security, *Environmental Sustainability*, **5** (3), 271–275. <https://doi.org/10.1007/s42398-022-00246-5>.
- Bailey, A. & Pitman, B. (2015) A Wealth of New Freely Downloadable Information on the Water Resources of South Africa, Swaziland and Lesotho, *Civil Engineering Magazine, South African Institution of Civil Engineering*, **23** (5), 13–18. https://saice.org.za/downloads/monthly_publications/2015/Civil-Engineering-June-2015.pdf.
- Barsalou, M. A. (2015) *Statistics for Six Sigma Black Belts*. Milwaukee: American Society for Quality, Quality Press.
- Braune, E. G. (2020) *A Stochastic, Daily Time-Step Model for the Conjunctive Use of Surface Water, Groundwater, Desalination and Water Reclamation for Municipalities*. Master's Dissertation, University of Stellenbosch, Stellenbosch, South Africa.
- Brutsaert, W., Cheng, L. & Zhang, L. (2020) Spatial distribution of global landscape evaporation in the early twenty-first century by means of a generalized complementary approach, *Journal of Hydrometeorology*, **21** (2), 287–298. <https://doi.org/10.1175/JHM-D-19-0208.1>.
- Celestin, S., Qi, F., Li, R., Yu, T. & Cheng, W. (2020) Evaluation of 32 simple equations against the Penman–Monteith method to estimate the reference evapotranspiration in the Hexi Corridor, Northwest China, *Water*, **12** (10), 2772. <https://doi.org/10.3390/w12102772>.
- Chapman, R. A., Midgley, G. F. & Smart, K. (2021) Diverse trends in observed pan evaporation in South Africa suggest multiple interacting drivers, *South African Journal of Science*, **117** (7/8), 1–7. <https://doi.org/10.17159/sajs.2021/7900>.
- Crago, R. D. & Brutsaert, W. H. (1992) A comparison of several evaporation equations, *Water Resources Research*, **28** (3), 951–954. <https://doi.org/10.1029/91WR03149>.
- Dlouhá, D., Dubovský, V. & Pospíšil, L. (2021a) Optimal calibration of evaporation models against Penman–Monteith equation, *Water*, **13**, 1484. <https://doi.org/10.3390/w13111484>.
- Dlouhá, D., Dubovský, V. & Pospíšil, L. (2021b) The evaporation estimation on lake most, *Multidisciplinary Aspects of Production Engineering*, **4** (1), 221–231. <https://doi.org/10.2478/mape-2021-0020>.
- Dubovský, V., Dlouhá, D. & Pospíšil, L. (2021) The calibration of evaporation models against the Penman–Monteith equation on lake most, *Sustainability*, **2021** (13), 313. <https://doi.org/10.3390/su13010313>.
- Finch, J. & Hall, R. (2001) *Estimation of Open Water Evaporation: A Review of Methods*. Bristol: Environment Agency.
- Han, Y., Calabrese, S., Du, H. & Yin, J. (2024) Evaluating biases in Penman and Penman–Monteith evapotranspiration rates at different timescales, *Journal of Hydrology*, **638** (2024), 131534. <https://doi.org/10.1016/j.jhydrol.2024.131534>.
- Jana, R. B., Ershadi, A. & McCabe, M. F. (2016) Examining the relationship between intermediate-scale soil moisture and terrestrial evaporation within a semi-arid grassland, *Hydrology and Earth System Sciences*, **20** (10), 3987–4004. <https://doi.org/10.5194/hess-20-3987-2016>.

- Jensen, M. E., Dotan, A. & Sanford, R., (2005) Penman-Monteith estimates of reservoir evaporation. In: Walton, P. E. (ed.) *Impacts of Global Climate Change*, Fort Collins, Colorado: American Society of Civil Engineers (ASCE) library, pp. 1–24. [https://doi.org/10.1061/40792\(173\)548](https://doi.org/10.1061/40792(173)548).
- Jerszurki, D., de Souza, J. L. M. & Silva, L. d. C. R. (2019) Sensitivity of ASCE-Penman–Monteith reference evapotranspiration under different climate types in Brazil, *Climate Dynamics*, **53**, 945–956. <https://doi.org/10.1007/s00382-019-04619-1>.
- Koudahe, K., Djaman, K. & Adewumi, J. K. (2018) Evaluation of the Penman–Monteith reference evapotranspiration under limited data and its sensitivity to key climatic variables under humid and semiarid conditions, *Modeling Earth Systems and Environment*, **4** (3), 1239–1257. <https://doi.org/10.1007/s40808-018-0497-y>.
- Leonard, L. (2023) Climate change, mining development and residential water security in the uMkhanyakude District Municipality, KwaZulu-Natal, South Africa: a double catastrophe for local communities, *Local Environment*, **28** (3), 331–346. <https://doi.org/10.1080/13549839.2022.2136644>.
- Linacre, E. T. (1977) A simple formula for estimating evaporation rates in various climates, using temperature data alone, *Agricultural Meteorology*, **18** (6), 409–424. [https://doi.org/10.1016/0002-1571\(77\)90007-3](https://doi.org/10.1016/0002-1571(77)90007-3).
- Lindauer, J., Byers, S., Lehn, G., Evans, E., Castendyk, D. & Moravec, B. (2023) A review of methods to calculate current and future evaporation rates from pit lakes with high concentrations of total dissolved solids. In: Abbasi, B., Parshley, J., Fourie, A. & Tibbett, M. (eds). *Mine Closure 2023*, Perth Australian Centre for Geomechanics. https://doi.org/10.36487/ACG_repo/2315_064.
- Loots, I., Colin Smithers, J. & Kjeldsen, T. R. (2023) Quantifying the influence of urban development on runoff in South Africa, *Urban Water Journal*, **20** (10), 1541–1554. <https://doi.org/10.1080/1573062X.2022.2027472>.
- Majidi, M., Alizadeh, A., Farid, A. & Vazifedoust, M. (2015) Estimating evaporation from lakes and reservoirs under limited data condition in a Semi-Arid Region, *Water Resources Management*, **29** (2015), 3711–3733. <https://doi.org/10.1007/s11269-015-1025-8>.
- Maidment, D. R. (1993) *Handbook of Hydrology*. New York: McGraw-Hill.
- Mercer, J. (2018) *Penman-Monteith and Priestley-Taylor Evaporation*. Available at: <https://wetlandscapes.github.io/blog/blog/penman-monteith-and-priestley-taylor/> [Accessed 16 June 2023].
- Meyer, A. F. (1944) *Evaporation From Lakes and Reservoirs*. St Paul, Minnesota: Minnesota Resources commission.
- Minitab® Statistical Software. (2024) *Minitab*. Chicago: Minitab.
- Miralles, D. G., Brutsaert, W., Dolman, A. J. & Gash, J. H. (2020) On the use of the term ‘evapotranspiration’, *Water Resources Research*, **56**, e2020WR028055. <https://doi.org/10.1029/2020WR028055>.
- Montgomery, D. C. & Runger, G. C. (2010) *Applied Statistics and Probability for Engineers*, 7th edn. Hoboken, New Jersey: John Wiley & Sons.
- Mouton, J. v. S., Loots, I. & Smithers, J. C. (2025) Development of appropriate synthetic design storms for small catchments in Gauteng, South Africa, *Journal of Water Management Modeling*, **33**, C535. <https://doi.org/10.14796/JWMM.C535>.
- Nevermann, H., Aminzadeh, M., Madani, K. & Shokri, N. (2024) Quantifying water evaporation from large reservoirs: implications for water management in water-stressed regions, *Environmental Research*, **262**, 119860. <https://doi.org/10.1016/j.envres.2024.119860>.
- Patel, J. N. & Majmundar, B. P. (2016) Development of evaporation estimation methods for a reservoir in Gujarat, India, *Journal-American Water Works Association*, **108** (9), E489–E500. <http://dx.doi.org/10.5942/jawwa.2016.108.0113>.
- Pillco Zolá, R., Bengtsson, L., Berndtsson, R., Martí-Cardona, B., Satgé, F., Timouk, F., Bonnet, M., Mollericon, L., Gamarra, C. & Pasapera, J. (2019) Modelling Lake Titicaca’s daily and monthly evaporation, *Hydrology and Earth System Sciences*, **23** (2), 657–668. <https://doi.org/10.5194/hess-23-657-2019>.
- Sabino, M. & de Souza, A. P. (2023) Global sensitivity of Penman–Monteith reference evapotranspiration to climatic variables in Mato Grosso, Brazil, *Earth*, **4**, 714–727. <https://doi.org/10.3390/earth4030038>.
- Santos, F. R. d., Wiecheteck, G. K., Virgens Filho, J. S. d., Carranza, G. A., Chambers, T. L. & Fekih, A. (2022) Effects of a floating photovoltaic system on the water evaporation rate in the passaúna reservoir, Brazil, *Energies*, **15**, 6274. <https://doi.org/10.3390/en15176274>.
- Schober, P., Boer, C. & Schwarte, L. A. (2018) Correlation coefficients: appropriate use and interpretation, *Anesthesia & Analgesia*, **126** (5), 1763–1768. <https://doi.org/10.1213/ANE.0000000000002864>.
- Schulze, R. E. (2011) *A 2011 Perspective on Climate Change and the South African Water Sector* (Report No. TT 518/12). Pretoria, South Africa: Water Research Commission.
- Schulze, R. E., Maharaj, M., Warburton, M. L., Gers, C. J., Horan, M. J. C., Kunz, R. P. & Clark, D. J. (2008) *South African Atlas of Climatology and Agrohydrology*. WRC Report No 1489/1/08. Pretoria, South Africa: Water Research Commission.
- Shuttleworth, W. J. (2007) Putting the ‘vap’ into evaporation, *Hydrology and Earth System Sciences*, **11** (1), 210–244. <https://doi.org/10.5194/hess-11-210-2007>.
- Smithers, J. C. & Schulze, R. E. (2003) *Design Rainfall and Flood Estimation in South Africa*. WRC Report No. 1060/1/03. Water Research Commission, Pretoria.
- Tabari, H., Grismer, M. E. & Trajkovic, S. (2013) Comparative analysis of 31 reference evapotranspiration methods under humid conditions, *Irrigation Science*, **31**, 107–117. <https://doi.org/10.1007/s00271-011-0295-z>.
- Tian, W., Liu, X., Wang, K., Bai, P. & Liu, C. (2021) Estimation of reservoir evaporation losses for China, *Journal of Hydrology*, **596**, 126142. <https://doi.org/10.1016/j.jhydrol.2021.126142>.
- Tian, W., Liu, X., Wang, K., Bai, P., Liu, C. & Liang, X. (2022) Estimation of global reservoir evaporation losses, *Journal of Hydrology*, **607**, 127524. <https://doi.org/10.1016/j.jhydrol.2022.127524>.

- Van Dijk, M. & van Vuuren, S. J. (2009) Destratification induced by bubble plumes as a means to reduce evaporation, *Water SA*, **35** (2), 158–167. <https://doi.org/10.4314/wsa.v35i2.76731>.
- Yaseen, Z. M., Al-Juboori, A. M., Beyaztas, U., Al-Ansari, N., Chau, K., Qi, C., Ali, M., Salih, S. Q. & Shahid, S. (2020) Prediction of evaporation in arid and semi-arid regions: a comparative study using different machine learning models, *Engineering Applications of Computational Fluid Mechanics*, **14** (1), 70–89. <https://doi.org/10.1080/19942060.2019.1680576>.
- Zhang, Y., Chiew, F. H., Peña-Arancibia, J., Sun, F., Li, H. & Leuning, R. (2017) Global variation of transpiration and soil evaporation and the role of their major climate drivers, *Journal of Geophysical Research: Atmospheres*, **122** (13), 6868–6881. <https://doi.org/10.1002/2017JD027025>.

First received 21 September 2025; accepted in revised form 22 January 2026. Available online 7 February 2026